International Journal of Pharmaceutics 362 (2008) 44–51

Contents lists available at ScienceDirect

International Journal of Pharmaceutics

journal homepage: www.elsevier.com/locate/ijpharm

Interaction of dipeptide prodrugs of saquinavir with multidrug resistance protein-2 (MRP-2): Evasion of MRP-2 mediated efflux

Ritesh Jain, Sheetal Agarwal, Nanda Kishore Mandava, Ye Sheng, Ashim K. Mitra*

Division of Pharmaceutical Sciences, School of Pharmacy, University of Missouri-Kansas City, 5005 Rockhill Road, Kansas City, MO 64110-2499, USA

ARTICLE INFO

Article history:
Received 4 June 2007
Received in revised form 4 June 2008
Accepted 5 June 2008
Available online 22 June 2008

Keywords:
Saquinavir
Multidrug resistance protein-2
Single pass intestinal perfusion
Intestinal absorption
P_{eff}
Effective intestinal permeability
Rat jejunum
Net water flux

ABSTRACT

Saquinavir (SQV), the first protease inhibitor approved by FDA to treat HIV-1 infection. This drug is a well-known substrate for multidrug resistance protein-2 (MRP-2). The objective of this study was to investigate whether derivatization of SQV to dipeptide prodrugs, valine-valine-saquinavir (Val-Val-SQV) and glycine-valine-saquinavir (Gly-Val-SQV), targeting peptide transporter can circumvent MRP-2 mediated efflux. Uptake and transport studies were carried out across MDCKII-MRP2 cell monolayers to investigate the interaction of SQV and its prodrugs with MRP-2. *In situ* single pass intestinal perfusion experiments in rat jejunum were performed to calculate intestinal absorption rate constants and permeabilities of SQV, Val-Val-SQV and Gly-Val-SQV. Uptake studies demonstrated that the prodrugs have significantly lower interaction with MRP-2 relative to SQV. Transepithelial transport of Val-Val-SQV and Gly-Val-SQV across MDCKII-MRP2 cells exhibited an enhanced absorptive flux and reduced secretory flux as compared to SQV. Intestinal perfusion studies revealed that synthesized prodrugs have higher intestinal permeabilities relative to SQV. Enhanced absorption of Val-Val-SQV and Gly-Val-SQV relative to SQV can be attributed to their translocation by the peptide transporter in the jejunum. In the presence of MK-571, a MRP family inhibitor, there was a significant increase in the permeabilities of SQV and Gly-Val-SQV indicating that these compounds are probably substrates for MRP-2. However, there was no change in the permeability of Val-Val-SQV with MK-571 indicating lack of any interaction of Val-Val-SQV with MRP-2. In conclusion, peptide transporter targeted prodrug modification of MRP-2 substrates may lead to shielding of these drug molecules from MRP-2 efflux pumps.

1. Introduction

Acquired immune deficiency syndrome (AIDS) is one of the infectious diseases reaching epidemic proportion. Millions of people are infected with human immunodeficiency virus (HIV) and the syndrome remains among the top five fatal diseases. Two different retroviruses, HIV-1 and HIV-2, cause HIV infection in humans (Rambaut et al., 2004). However, HIV-1 is responsible for the majority of infections globally. Inclusion of HIV protease inhibitors (PIs) in 'highly active antiretroviral therapy' (HAART) has substantially improved clinical outcomes of AIDS patients (Wilson et al., 2007; Wood et al., 2007). However, complete eradication of HIV infection still remains an elusive goal. Protease inhibitors (PIs) are considered to be the most important therapeutic agents to date for the treatment of HIV infection. Currently available PIs approved by FDA for AIDs include saquinavir (SQV), ritonavir, indinavir, nelfinavir, lopinavir, amprenavir, fosamprenavir, atazanavir and tipranavir. Protease inhibitors bind to the active site of the HIV protease and inhibit the replication of HIV (Deeks et al., 1997; Flexner, 1998). Despite high anti-HIV activity of these agents, several unfavorable pharmacokinetic parameters, i.e. plasma protein binding, low solubility, high metabolism and cellular efflux limit their efficacy (Lin et al., 1995, 1996; Chiba et al., 1997; Sudoh et al., 1998). Most of the PIs are also substrates for P-glycoprotein (P-gp) and multidrug drug resistance proteins (MRPs). Recently it has been shown that these membrane transporters play an important role in oral absorption of these therapeutic agents (Kim et al., 1998a,b; Lee and Gottesman, 1998; Lee et al., 1998; Williams et al., 2002).

Saquinavir exhibits low and variable oral bioavailability ranging from 4 to 16% (Schapiro et al., 1996; Williams and Sinko, 1999). Several reports speculate that low and variable oral bioavailability of SQV and other PIs is primarily due to their efflux by membrane bound efflux pumps like P-glycoprotein and multi drug resistance proteins (MRPs) and partly due to CYP3A4 mediated metabolism (Dupre et al., 1995; Fitzsimmons and Collins, 1997; Kim et al., 1998a,b; Polli et al., 1999; Williams et al., 2002). Previous reports have delineated the role of P-gp (ABCB1) in causing low and variable permeability of these agents. In recent years the role of MRP-2

* Corresponding author. Tel.: +1 816 235 1615; fax: +1 816 235 5779.
E-mail address: mitraa@umkc.edu (A.K. Mitra).

0378-5173/$ – see front matter © 2008 Elsevier B.V. All rights reserved.
doi:10.1016/j.ijpharm.2008.06.013

(ABCC2) in drug disposition has been widely studied and clinical implications of this efflux transporter are escalating (Morrow et al., 2000; Payen et al., 2002; Su et al., 2004).

MRP-2 was characterized functionally as a multispecific organic anion transporter in bile canalicular membrane of rat hepatocytes (Jansen et al., 1993). MRP-2 belongs to the MRP family and nine isomers have been identified in this family. MRP-2 is a 1545 amino acid, 190 kDa protein having 2 ATP binding domains and 17 transmembrane regions in its sequence. In rat intestine, MRP-2 is highly expressed on the brush border membrane of the proximal segments, and the expression gradually decreases from the jejunum to the distal ileum (Mottino et al., 2000; Rost et al., 2002). Also MRPs are present on blood brain barrier (BBB) and play a significant role *in vivo* in the absorption of SQV across BBB (Park and Sinko, 2005). MRP-2 can efflux glucuronide, glutathione and sulfate conjugate of many endogenous substrates and xenobiotics. In addition to conjugated endogenous metabolite, MRP-2 causes efflux of a wide range of unconjugated organic anions, some of which are clinically important drugs (Haimeur et al., 2004). MRP-2 has also been shown to actively efflux drugs like methotrexate, irinotecan, ampicillin, pravastatin and grepafloxacin (Haimeur et al., 2004). Recently it has been shown that several HIV PIs (saquinavir, ritonavir, lopinavir, amprenavir and indinavir) are substrates of MRP-2 (Huisman et al., 2002). MRP-2 is functionally similar to P-gp and plays an important role as an efflux pump in drug absorption across the intestine and BBB.

In a previous report, we have demonstrated that prodrug modification of SQV to valine-valine-saquinavir (Val-Val-SQV) and glycine-valine-saquinavir (Gly-Val-SQV) targeted towards peptide transporter resulted in circumvention of P-gp mediated cellular efflux (Jain et al., 2005). Such circumvention consequently resulted in enhanced permeabilities of SQV prodrugs Val-Val-SQV and Gly-Val-SQV across MDCKII-MDR1 cells and rat intestine (Jain et al., 2005, 2007). Such enhanced permeabilities may be attributed to evasion of P-gp mediated efflux and utilization of peptide transporter. In continuation of our previous report, the major objective of the present study was to investigate whether prodrug modification of SQV to Val-Val-SQV and Gly-Val-SQV can result in the circumvention of MRP-2 mediated efflux. To test this hypothesis *in vitro* uptake and transport studies were conducted across MDCKII-MRP2 cells that have been genetically engineered to express high levels of MRP-2. Further, *in situ* single pass intestinal perfusion (SPIP) studies were carried out to study the disposition of these agents across rat jejunum. SPIP is a well-established technique employed to study intestinal drug absorption. In this technique, a known concentration of drug is perfused through a section of the jejunum with intact blood supply. Disappearance of drug from the perfusate is attributed to intestinal absorption (Cummins et al., 2003; Berggren et al., 2004). MK-571, a specific MRP family inhibitor was added to the perfusate to delineate the role of MRP-2 in the intestinal absorption of SQV and its peptide prodrugs.

2. Experimental

2.1. Materials

Saquinavir mesylate was generously supplied by Hoffmann-La Roche. All the prodrugs used in the study were synthesized according to previously published procedure from our laboratory (Jain et al., 2005). [^{3}H] Saquinavir (1.0 Ci/mmol) was obtained from Moravek Biochemicals (Brea, CA). [^{14}C] Mannitol was purchased from Biomedical Inc. (Aurora, OH). MDCK cells, retrovirally transfected with the human *MRP2* cDNA (MDCKII-MRP2) were donated by Dr. Piet Borst (Netherlands Cancer Institute, Amsterdam). The Dulbecco's Modified Eagle Medium (DMEM), fetal bovine serum, minimum essential medium and non-essential amino acids were obtained from Gibco (Invitrogen, Grand Island, NY). Penicillin, streptomycin, sodium bicarbonate, and HEPES were purchased from Sigma Chemical (St. Louis, MO). Culture flasks (75 cm^2 growth area), polyester Transwell® (pore size 0.4 μM and 12 mm diameter) and 12-well plates were obtained from Costar (Cambridge, MA). Buffer components and other solvents were procured from Fisher Scientific Co. (Fair Lawn, NJ).

2.2. Cell culture

MDCKII-MRP2 cells (passages 4–15) were cultured at 37 °C in a humidified atmosphere with 5% CO_2. Confluency was assessed by light microscopy. Cells were passaged at 70–80% confluency using 0.25% trypsin-EDTA and were seeded at a density of 50,000 cells/cm^2 on 12-well tissue culture plates or on collagen coated Transwell® inserts and were maintained in DMEM, supplemented with 10% fetal bovine serum, 100 IU/mL penicillin, 100 μg/mL streptomycin, 1% (v/v) non-essential amino acid, 3.7 g of sodium bicarbonate and 10 mM HEPES, pH 7.4. Cells were allowed to grow for 5–8 days. Integrity of monolayers formed on transwell plates were evaluated by monitoring [^{14}C] mannitol permeability and transepithelial electric resistance (TEER), with EVOM (epithelial volt ohmmeter; World Precision Instruments, Sarasota, FL). TEER values of the cell monolayers were approximately 250 Ω cm^2 after correcting for the resistance imparted by filters. [^{14}C] mannitol transport was <0.5% per hour (Papp $<2 \times 10^{-7}$ cm/s) across the cell monolayers.

2.2.1. Uptake studies

Uptake studies were conducted with confluent cell monolayers, 6–8 days post-seeding. Medium was aspirated and cells were washed three times with DPBS pH 7.4. SQV, Val-Val-SQV and Gly-Val-SQV test solutions were prepared prior to conducting the experiments. Concentrated stock solutions of SQV and its prodrugs were prepared in DMSO. Test solutions were prepared by dilution with DPBS pH7.4. Final DMSO concentration in all experiments was maintained constant at 0.5% (v/v) or less. The experiment was initiated by adding 1 mL drug solution (in the presence or absence of competing substrates) to the well. Incubation was carried out over a period of 10 min at 37 °C. At the end of incubation period, drug solution was removed and the cell monolayer was washed three times with ice-cold stop solution. Cells were lysed overnight (1 mL 0.1%, w/v) Triton X-100 in 0.3N sodium hydroxide) at room temperature. Aliquots (500 μL) were withdrawn from each well and transferred to scintillation vials containing 5 mL scintillation cocktail. Samples were then analyzed by liquid scintillation spectrophotometry with a Beckman scintillation counter (Model LS-6500, Beckman Instruments, Inc.). Uptake data was normalized to the protein content of each well. Amount of protein in the cell lysate was quantified by Bradford method utilizing BioRad protein estimation kit (BioRad, Hercules, CA).

2.2.2. Transport studies

Transport studies were conducted with MDCKII-MRP2 cell monolayers grown for 6–7 days on 12-well transwell inserts (diameter 12 mm). The medium was aspirated and cell monolayers washed three times (10 min each wash) with DPBS pH 7.4 before conducting an experiment. Volumes of the apical and basolateral chambers were maintained at 0.5 and 1.5 mL, respectively. Transport experiments were conducted for a period of 3 h. Donor concentrations used in the bidirectional transport studies were SQV 22 μM, SQV + MK571 28 μM, Gly-Val-SQV 56 μM, Gly-Val-SQV + MK571 64 μM, and Val-Val-SQV 37 μM, Val-

Val-SQV + MK571 38 μM. Aliquots (200 μL) were withdrawn at predetermined time intervals, i.e. 15, 30, 45, 60, 90, 120, 150, 180 min, respectively, and replaced with fresh DPBS pH 7.4 to maintain sink conditions. Dilutions were taken into account for the calculations. Samples were stored at −80 °C until further analysis. All transport experiments were performed at 37 °C.

2.3. Intestinal perfusion solution

The composition of the perfusate solution was NaCl (48 mM), KCl (5.4 mM), Na_2HPO_4 (28 mM), NaH_2PO_4 (43 mM), mannitol (35 mM), polyethylene glycol (PEG 4000; 1 g/L) and D-glucose (10 mM). Solution pH and osmolality were maintained at 6.5 and 290 mOsm/L, respectively (Fagerholm et al., 1996; Issa et al., 2003).

2.4. Adsorption and stability of drug/prodrug

Briefly solutions of SQV and prodrugs (25 μM) in distilled, deionized water were incubated at 37 °C with the tubings for 2 h. Samples were collected at appropriate time intervals and analyzed by HPLC. No drug adsorption on the tube and glass surfaces was observed. Stability studies of SQV and its prodrugs (25 μM) were also conducted in intestinal perfusion buffer. All the compounds were incubated in the perfusion buffer for 2 h at 37 °C. Samples were collected at predetermined time points and analyzed by HPLC to monitor any drug degradation.

2.5. Rat single-pass intestinal perfusion technique

All intestinal perfusion studies were carried out with jejunum segments from male Sprague–Dawley rats (200–250 g). Animal studies were performed in accordance with a protocol approved by the IACUC at the University of Missouri-Kansas City. Animals were fasted for 14–20 h (water *ad libitum*) prior to initiation of a perfusion experiment. The surgery for SPIP of the rat jejunum was performed as described in details elsewhere (Berggren et al., 2004). Briefly, rats were anesthetized and the abdomen was opened with a midline longitudinal incision. A jejunal segment of approximately 10 cm was measured and cannulated with plastic tubing (4 mm oD, inlet tube 40 cm, outlet tube 25 cm). Care was taken to avoid injury to local circulatory system. Intestinal segment was rinsed with intestinal perfusate maintained at 37 °C for approximately 30 min until the outlet solution was visually clear. A bolus dose of 3–5 mL drug solution was introduced and then allowed to equilibrate with intestinal segment. Thereafter the jejunum segment was perfused at a constant flow rate (Q_{in}) of 0.2 mL/min with a peristaltic pump (Ismatec pump, Cole Parmer Instrument Co., IL) Each perfusion experiment lasted for 120 min and samples were collected at an interval of every 15 min in pre-weighed glass tubes. All perfusate samples collected were weighed and stored at −80 °C until analysis. At the end of an experiment, animals were euthanized with a cardiac injection of saturated potassium chloride solution. Finally, at the end of an experiment, the intestine (jejunum) was removed and length of intestine was measured. The radius of the intestine was taken to be 0.18 cm (Issa et al., 2003).

2.6. Sample preparation

Transport samples were analyzed with LC–MS/MS. Sample preparation was carried out by a liquid–liquid extraction technique (Proust et al., 2000). Briefly, to a 200 μL sample 100 μL internal standard was added. The samples were vortexed and 250 μL of 0.05 mol/L sodium hydroxide was added to the solution. This mixture was vortexed and 500 μL of methyl-*t*-butyl ether was added. Again the samples were vortexed for 1 min and centrifuged at 2500 × *g* for 5 min. Samples were kept at −20 °C for 20 min to freeze the aqueous layer. Methyl-*t*-butyl ether layer was decanted and samples were dried in vacuum. The residue was reconstituted in 200 μL of water, and 50 μL of the reconstituted extract was injected onto the LC–MS/MS for analysis. Standard solutions in buffer were also extracted and quantified following a similar procedure described previously. Extraction efficiencies for drug and prodrugs were found to be 80% (±5%). Extraction efficiency for internal standard was 90% (±6%). All the extractions were carried out in triplicates and compared with calibration standards.

2.7. Analytical procedure

2.7.1. HPLC analysis

SQV, Val-Val-SQV and Gly-Val-SQV samples obtained from intestinal perfusion experiments were analyzed by a reversed phase HPLC technique (Ucpinar and Stavchansky, 2003). The HPLC system was comprised of a HP 1050 pump, Waters dual wavelength absorbance UV detector, and an Alcott auto sampler (model 718AL HPLC). A C(8) Luna column (250 mm × 4.6 mm; Phenomenex, Torrance, CA) was employed for the separation of analytes. Mobile phase was composed of acetonitrile:water:triethylamine (55:44:1%; v/v/v) and pH was adjusted to 6.5 with phosphoric acid. Flow rate was maintained at 0.8 mL/min and detection wavelength was set at 240 nm. Elution times for SQV, Gly-Val-SQV and for Val-Val-SQV were 8.6 and 12 min, respectively. Precision and accuracy of the assay were determined by analyzing replicate standard samples ($n = 3$) at low, medium and high concentration ranges. Precision was expressed as coefficient of variation (CV%) and accuracy was determined as [(average analyte concentration calculated)/(known concentration) × 100%]. Assay precision ranged from 4.5 to 10.2% CV and accuracy varied from 85.0 to 115.0% of known concentrations (data not shown).

2.7.2. LC–MS/MS analysis

Samples from transport studies were analyzed by a QTrap® LC/MS/MS mass spectrometer (Applied Biosystems, Foster City, CA, USA) equipped with Agilent 1100 Series quaternary pump (Agilent G1311A), vacuum degasser (Agilent G1379A) and auto sampler (Agilent G1367A, Agilent Technology Inc., Palo Alto, CA, USA). HPLC separation was performed on a Luna C 18(2) column 100 mm × 2.0 mm, 3 μm (Phenomenex, Torrance, CA). The mobile phase (35% ACN and 65% of 0.1% TFA in Water) was run at a flow rate of 0.2 mL/min.

The sample volume injected was 50 μL and the analysis time was 4–6 min. Electrospray ionization in the positive mode was applied in the sample introduction and the detection was operated in the multiple-reaction monitoring (MRM) mode. Precursor ion of analytes and internal standard were determined from spectra obtained during the infusion of standard solutions with an infusion pump connected directly to the electrospray source. As a result of very soft ionization, provided by electrospray ion source, only singly charged molecular ions were observed. Each of these precursor ions was subjected to collision-induced dissociation to determine the product ions. The precursor and the product ions generated were; SQV + 671.4/266.4; Val-Val-SQV + 869.5/266.4; Gly-Val-SQV + 827/266.4; Val-SQV + 770.5/266.4 and verapamil (IS) + 455/150. The turbo ion spray setting and collision gas pressure were optimized (IS Voltage: 5500 V, temperature: 350 °C, nebulizer gas: 40 psi, curtain gas: 40 psi). MS/MS was performed using nitrogen as the collision gas. Other ion source parameters were: declustering potential (DP): 96 V; collision energy (CE): 75 V: entrance potential (EP) 8.5 V; and collision cell exit potential (CXP) 4 V. Peak areas for all components were automatically integrated by using Analyst™ software, and peak–area ratios (area of ana-

lytes to area of IS) were plotted versus concentration by weighted linear regression (1/concentration). Analytical data from prodrugs with MRM method shows significant linearity that extends to picomolar range. The limits of quantification were found to be SQV, 5 ng/mL; Val-SQV, 15 ng/mL; Val-Val-SQV, 15 ng/mL and Gly-Val-SQV, 15 ng/mL. Assay precision ranged from 5.0 to 13.0% CV and accuracy varied from 80.0 to 110.0% of known concentrations. This method generated rapid and reproducible results.

2.8. Data analysis

2.8.1. Transport studies

Cumulative amounts of prodrugs (Val-Val-SQV or Gly-Val-SQV) and the parent drug SQV, generated during transport across the cell monolayers were plotted as a function of time to determine flux and permeability coefficients. Linear regression of the amounts transported as a function of time yielded the rate of transport across the cell monolayer (dM/dt). Rate divided by the cross-sectional area available for transport (A) generated the steady state flux as shown in Eq. (1).

$$\text{Flux} = \frac{(dM/dt)}{A} \quad (1)$$

In all the transport studies, slopes obtained from the linear portion of the curve were used to calculate permeability values. Permeability was calculated by normalizing the steady state flux to the donor concentration (C_d) of the drug or prodrug according to Eq. (2).

$$\text{Permeability Coefficient} = \frac{\text{Flux}}{C_d} \quad (2)$$

2.8.2. Calculation of absorption rate constant (k_a)

Prodrug/drug concentrations obtained from the perfusate samples were corrected for changes in water flux during each time interval. Density corrected gravimetric method was utilized for the calculation of net water flux across the intestinal segment (Sutton et al., 2001; Issa et al., 2003). The advantage of this method over the usage of non-absorbable markers (like phenol red and ^{14}C polyethylene glycols) is that it does not interfere with analytical method and does not pose any radiation safety issues. The density of collected samples was determined by weighing the contents using an electronic weighing balance of a known volume of perfusate. Net water flux (NWF) was calculated by using Eq. (3)

$$\text{NWF} = \left[1 - \frac{Q_{out}}{Q_{in}}\right] \times \frac{Q_{in}}{l} \quad (3)$$

Q_{in} is the measured flow rate (mL/min) of entering intestinal perfusate, Q_{out} is the measured flow (mL/min) of exiting intestinal perfusate for the specified time interval calculated from the actual intestinal perfusate density (g/mL), l is the length (cm) of intestinal segment perfused.Absorption rate constant k_a and $C_{out(corr)}$ were calculated from the Eq. (4) and (5)

$$k_a = \left(1 - \frac{C_{out(corr)}}{C_{in}}\right) \times \frac{Q}{V} \quad (4)$$

and

$$C_{out(corr)} = C_{out} \times \frac{Q_{out}}{Q_{in}} \quad (5)$$

$C_{out(corr)}$ is the water flux corrected concentration of the compound measured in the exiting perfusate at the specified time interval (45, 60, 75, 90, 105, 120 min); C_{in} denotes drug concentration measured in entering perfusate; Q is the perfusion rate (~0.2 mL/min); and V is the volume of perfused segment.

2.8.3. Drug permeability measurement across jejunum

The single pass intestinal perfusion method is based on reaching steady state with respect to diffusion of compound across the intestinal segment. Steady state is confirmed by plotting the ratio of the outlet to inlet concentrations (corrected for water transport) versus time. Permeability calculations across rat jejunum (P_{eff}) were performed from intestinal perfusate samples collected over 45–120 min (steady state). P_{eff} of SQV, Vall-Val-SQV and Gly-Val-SQV was calculated from Eq. (6)

$$P_{eff} = \frac{-Q_{in} \times \ln(C_{out(corr)}/C_{in})}{A} \quad (6)$$

Q_{in} is the flow rate (mL/min) of entering perfusate, $C_{out(corr)}$ is the water flux corrected concentration of the permeant in the exiting perfusate, C_{in} denotes drug concentration in entering perfusate, A is the surface area (cm^2) of the perfused intestinal segment.

2.9. Statistical analysis

All experiments were conducted at least in triplicate and results are expressed as mean ± S.E.M/S.D. Statistical comparison of mean values were performed with one-way analysis of variance (ANOVA) or Student t-test (Graph Pad INSTAT, Version 3.1). $^{*}p < 0.05$ was considered to be statistically significant.

3. Results

3.1. Interaction of SQV, Val-Val-SQV and Gly-Val-SQV with MRP-2 in MDCKII-MRP2 cells

Uptake of [^{3}H] SQV (0.5 μCi/mL), by MDCKII-MRP2 cells, was studied in the presence of equimolar concentration (50 μM) of SQV, Val-Val-SQV, Gly-Val-SQV and MK-571 (MRP-2 inhibitor). A 4-fold increment in the cellular uptake of [^{3}H] SQV was observed in the presence of 50 μM MK-571. This enhanced uptake is probably due to inhibition of MRP-2 mediated cellular efflux of [^{3}H] SQV. Also a significant elevation in cellular uptake of [^{3}H] SQV was observed in the presence of SQV and its prodrugs (Fig. 1). However, the extent of MRP-2 inhibition differed between SQV and its prodrugs. In the presence of SQV (50 μM) a 3.3-fold increase in cellular uptake of [^{3}H] SQV was observed (Fig. 1). However, in the presence of Val-Val-SQV (50 μM) and Gly-Val-SQV (50 μM), only 1.9- and 2.5-fold increase in cellular uptake of [^{3}H] SQV, respectively, were noted. These results indicate that prodrug modification resulted in reduced affinity of the prodrug molecule towards MRP-2.

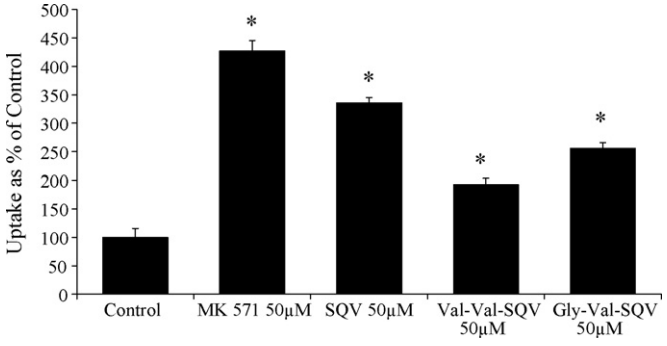

Fig. 1. Cellular uptake of [^{3}H] SQV (0.5 μCi/mL) by MDCKII-MRP2 cell monolayers in the absence (control) and presence of MK571, SQV, Val-Val-SQV and Gly-Val-SQV. Increased uptake [^{3}H] SQV was observed in presence of SQV and prodrugs. Statistically significant difference ($^{*}p < 0.05$) was observed in uptake as compared to control. Values are mean ± S.D. ($n = 4$).

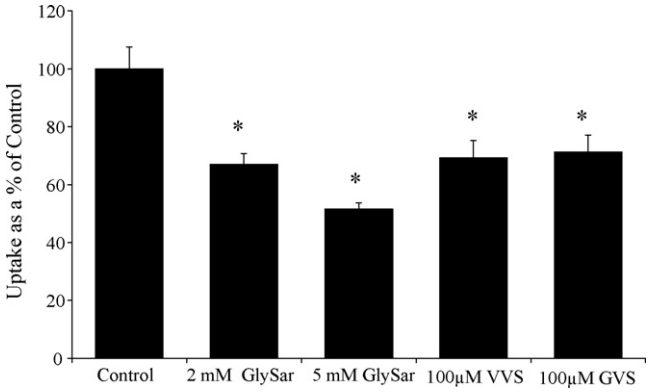

Fig. 2. Uptake of [^{3}H] gly-sar (0.5 μci/mL) by MDCKII-MRP2 cells in the absence (control) or presence of 2 and 5 mM unlabeled gly-Sar, Gly-Val-SQV (100 μM), and Val-Val-SQV (100 μM). ($^*p < 0.05$) represents statistically significant difference as compared to control. Data expressed as mean ± S.D. ($n = 4$).

3.2. Uptake of [^{3}H] Gly-Sar in the presence of Val-Val-SQV and Gly-Val-SQV by MDCKII-MRP2 cells

Interaction of Val-Val-SQV and Gly-Val-SQV with peptide transporter was studied in MDCKII-MRP2 cells. Uptake of [^{3}H] gly-sar (0.5 μCi/mL), in the presence of unlabeled gly-sar, at concentrations of 2 and 5 mM, demonstrated a concentration dependent reduction in cellular accumulation of [^{3}H] gly-sar (Fig. 2). Unlabeled gly-sar at concentrations of 2 and 5 mM reduced the uptake of [^{3}H] gly-sar by 33 and 49%, respectively. However, such [^{3}H] gly-sar uptake was significantly inhibited in the presence of Val-Val-SQV (100 μM) and Gly-Val-SQV (100 μM). Also, in our previous report we have shown that SQV itself does not interact with [^{3}H] gly-sar (Jain et al., 2005). These results indicate that the synthesized prodrugs probably interact with peptide transporter expressed on MDCKII-MRP2 cells. A larger percentage inhibition of [^{3}H] gly-sar uptake inhibition by SQV prodrugs, compared to equimolar concentrations of unlabeled gly-sar, indicates that SQV prodrugs may possess even higher affinity for the peptide transporter relative to gly-sar, a well known peptide transporter substrate.

3.3. Transport of SQV across MDCKII-MRP2 cells

Bidirectional transport of SQV across MDCKII-MRP2 cells revealed that transport of SQV in the absorptive direction, apical to basolateral (A → B), was significantly lower than that in secretory direction, basolateral to apical (B → A) direction (Fig. 3). Apparent permeability A → B (P_{app}) of SQV was $0.93 \pm 0.28 \times 10^{-6}$ and B → A direction $6.83 \pm 0.57 \times 10^{-6}$ cm s^{-1}. Efflux ratio, which is defined as the ratio of apparent permeabilities in B → A to A → B direction (P_{app} B → A/P_{app} A → B), was determined to be 7.4 for SQV. This asymmetric permeation is due to the involvement of an apically polarized MRP-2 efflux transporter, for which SQV is an excellent substrate. In the presence of 100 μM MK-571, a specific MRP-2 inhibitor, absorptive permeability (P_{app}) of SQV significantly enhanced from $0.93 \pm 0.28 \times 10^{-6}$ to $4.39 \pm 0.56 \times 10^{-6}$ cm s^{-1} (Fig. 3). This enhanced absorptive permeability of SQV in the presence of MK-571 was due to the complete blockade of apically localized MRP-2 efflux pump by MK-571. The efflux ratio in the presence of MK-571 was reduced to 1.3. These results clearly indicate that SQV is an excellent substrate for MRP-2 and inhibition of MRP-2 mediated efflux process can lead to enhanced transport of SQV into MDCKII-MRP2 cells.

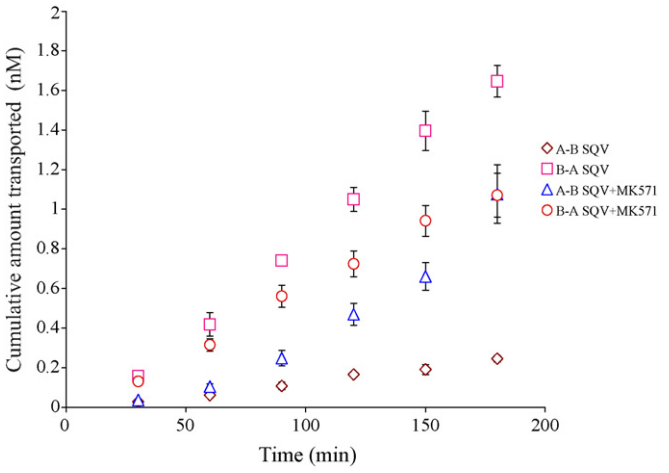

Fig. 3. Bidirectional transepithelial transport of SQV across MDCKII-MRP-2 cell monolayers: (◊) apical to basolateral (AP-BL) direction; (□) basolateral to apical (BL-AP) direction; (△)AP-BL transport in presence of MK-571; (○) BL-AP transport in presence of MK-571. Values are expressed as mean ± S.D. ($n \geq 3$).

3.4. Transport of Val-Val-SQV and Gly-Val-SQV across MDCKII-MRP2 cells

Transport of Val-Val-SQV and Gly-Val-SQV were carried out across MDCKII-MRP2 cell monolayer to investigate the interaction of prodrugs with MRP-2 efflux transporter. Cumulative amounts of drug transported (the sum of prodrug and regenerated parent drug) were plotted as a function of time. Apparent permeabilities (P_{app}) were determined from the linear portion of the cumulative amounts transported versus time plots. Translocation of Val-Val-SQV across MDCKII-MRP2 cells revealed that there was a significant rise in apparent permeability of Val-Val-SQV ($1.51 \pm 0.11 \times 10^{-6}$ cm s^{-1}) in the apical to basolateral (A → B) direction relative to SQV ($0.93 \pm 0.28 \times 10^{-6}$ cm s^{-1}) (Fig. 4). Such enhanced A → B transport can be due to partial circumvention of MRP-2 mediated efflux and binding and translocation of the prodrugs by the peptide transport system. Moreover, basolateral to apical transport (B → A) of Val-Val-SQV ($3.24 \pm 0.51 \times 10^{-6}$ cm s^{-1}) diminished significantly relative to SQV ($6.83 \pm 0.57 \times 10^{-6}$ cm s^{-1}). Such decrease in B → A transport may be due to reduced affinity of Val-Val-SQV for MRP-2. The efflux ratio for Val-Val-SQV was calculated to be 2.1 (Fig. 4). Further transport studies of Val-Val-SQV in the presence of MK-571 (100 μM) revealed that there was no significant change in A → B

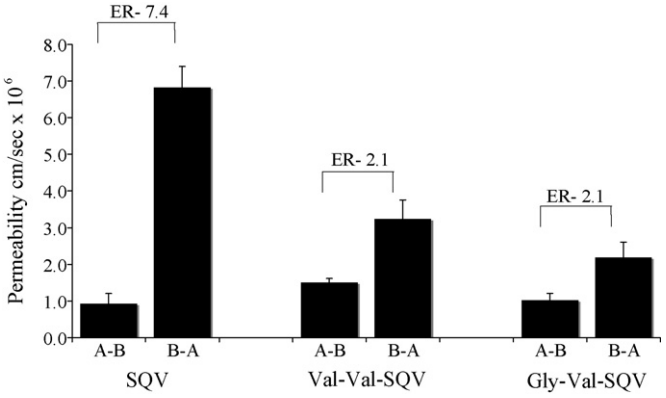

Fig. 4. Apparent permeability of SQV, Val-Val-SQV and Gly-Val-SQV in Apical to Basolateral direction (A–B) and Basolateral to Apical direction (B–A) across MDCKII-MRP2 cells. ER represent efflux ratio. Data expressed as mean ± S.D. ($n \geq 3$).

Table 1
Permeabilities of SQV, Val-Val-SQV and Gly-Val-SQV across MDCKII-MRP2 cells

Compounds	Permeability A → B ($\times 10^6$ cm s^{-1})	Permeability B → A ($\times 10^6$ cm s^{-1})
SQV	0.93 ± 0.28	6.83 ± 0.57
SQV + MK571	4.39 ± 0.56*,†	5.79 ± 0.48
Val-Val-SQV	1.51 ± 0.11*	3.24 ± 0.51*
Val-Val-SQV + MK571	1.67 ± 0.11*	3.65 ± 0.25*
Gly-Val-SQV	1.02 ± 0.19	2.19 ± 0.42*
Gly-Val-SQV + MK571	1.50 ± 0.12*	1.75 ± 0.09*,†

Values are expressed as mean ± S.D.
* $p < 0.05$ as compared to SQV.
† $p < 0.05$ in presence of MK-571.

and B → A permeability values confirming that Val-Val-SQV interaction with MRP-2 efflux pump is minimal (Table 1). Also the efflux ratio of Val-Val-SQV remained unchanged in the presence of MK-571 confirming that prodrug modification of SQV to Val-Val-SQV completely abolished its interaction with MRP-2 (Fig. 5).

Gly-Val-SQV also demonstrated slight elevation in A → B permeability as compared to SQV (Fig. 4). However, the difference was not statistically significant. In the presence of MK-571 there was a significant increase in the permeability values, of Gly-Val-SQV, in apical to basolateral (A → B) direction relative to SQV, indicating that Gly-Val-SQV interacts with MRP-2 (Table 1). This observation was further confirmed by comparing the efflux ratio of Gly-Val-SQV in the absence and presence of MK-571. In the absence of MK-571 the efflux ratio was 2.1 and in the presence of MK-571 the efflux ratio reduced to 1.1(Fig. 5). Such lowering in efflux ratio may be attributed to the inhibition of MRP-2 mediated efflux by MK-571. These results are consistent with our earlier observations that Gly-Val-SQV enhanced cellular uptake of [^{3}H] saquinavir to a greater extent relative to Val-Val-SQV in MDCKII-MRP2 cells.

3.5. Adsorption studies

These studies were carried out to ensure that drug loss during SPIP is due to absorption only and not due to other processes (e.g. non-specific binding to the tubing or chemical degradation). No loss of SQV, Val-Val-SQV and Gly-Val-SQV was observed during the perfusion of solutions through the tubings. Both SQV and prodrugs were also found to be stable in perfusion buffer as well as intestinal perfusate at 37 °C for 2 h (data not shown).

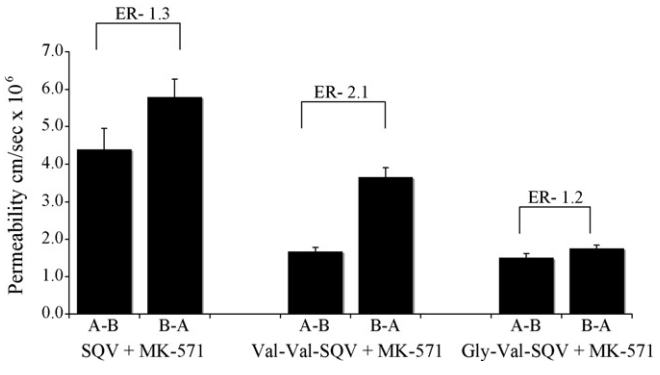

Fig. 5. Apparent permeability of SQV + MK-571, Val-Val-SQV + MK-571 and Gly-Val-SQV + MK-571 in Apical to Basolateral direction (A–B) and Basolateral to Apical (B–A) direction across MDCKII-MRP2 cells. ER represent efflux ratio. Data expressed as mean ± S.D. ($n \geq 3$).

Table 2
Absorption rate constant k_a and permeabilities of SQV, Val-Val-SQV and Gly-Val-SQV across rat jejunum

Compounds	Rat intestinal absorption rate constant, k_a ($\times 10^3$ min^{-1})	Rat intestinal permeability ($\times 10^5$ cm s^{-1})
SQV	14.1 ± 3.4	2.3 ± 0.6
SQV + MK-571	64.1 ± 15.1*,†	11.6 ± 3.0*,†
Gly-Val-SQV	25.6 ± 5.7	4.2 ± 1.0
Gly-Val-SQV + MK-571	50.4 ± 4.1*,†	9.0 ± 0.7*,†
Val-Val-SQV	65.8 ± 4.3*	12.9 ± 1.7*
Val-Val-SQV + MK-571	61.0 ± 8.0	11.6 ± 0.9

Values are expressed as mean ± S.E. #Control values were adapted (Jain et al., 2007).
* $p < 0.05$ as compared to SQV.
† $p < 0.05$ in presence of MK-571.

3.6. Rat single pass intestinal perfusion of SQV and its prodrugs

In situ single pass intestinal perfusion experiments in rat jejunum were performed to determine absorption rate constants and intestinal permeabilities of SQV, Val-Val-SQV and Gly-Val-SQV. Equimolar (25 μM) concentrations of SQV, Val-Val-SQV and Gly-Val-SQV were prepared for perfusion studies. Intestinal permeability values of SQV, Val-Val-SQV and Gly-Val-SQV across rat jejunum were calculated to be $2.3 \pm 0.6 \times 10^{-5}$, $4.2 \pm 1.0 \times 10^{-5}$ and $12.9 \pm 1.7 \times 10^{-5}$ cm s^{-1}, respectively (Table 2). Steady state fluxes of SQV, Val-Val-SQV and Gly-Val-SQV in the presence of MK-571 (100 μM) are shown in Fig. 6. In the presence of MK-571 (100 μM) intestinal permeability and absorption rate constant of SQV and Gly-Val-SQV significantly increased, indicating that these compounds are substrates for MRP-2 (Fig. 7). However, MK-571 had no effect on the absorption rate constant and permeability of Val-Val-SQV demonstrating that Val-Val-SQV probably does not interact with MRP-2 efflux pump (Table 2). Moreover, Val-Val-SQV exhibited highest absorption rate constant and intestinal permeability in comparison to SQV and Gly-Val-SQV. These results clearly show that Val-Val-SQV is a more effective prodrug than Gly-Val-SQV in bypassing efflux pumps. The results are consistent with the previous *in vitro* uptake and transport studies where Val-Val-SQV exhibited least interaction with MRP-2. Thus enhanced permeability of Val-Val-SQV across rat jejunum may be due to peptide transporter mediated translocation and possible circumvention of MRP-2 mediated efflux.

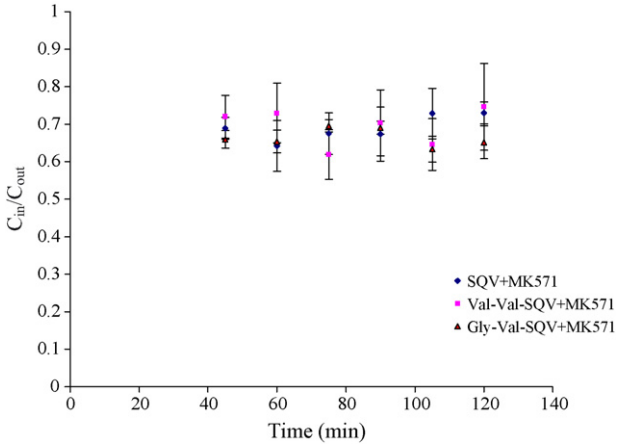

Fig. 6. Steady state flux of SQV + MK-571, Val-Val-SQV + MK-571, Gly-Val-SQV + MK-571 exiting the luminal perfusate. Values are expressed as mean ± S.E. ($n \geq 3$).

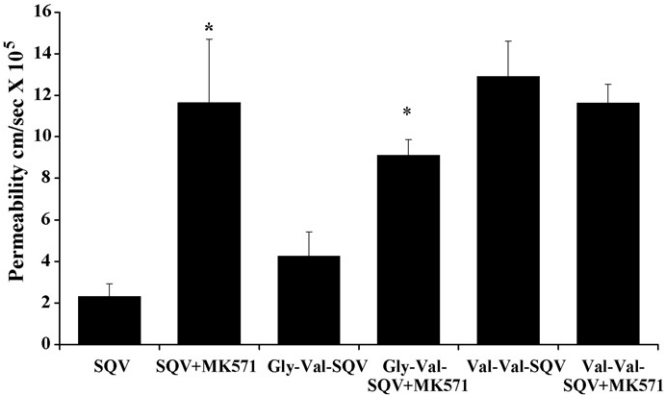

Fig. 7. Permeabilities of SQV, Val-Val-SQV and Gly-Val-SQV in presence and absence of MK-571 across rat jejunum. Values are expressed as mean ± S.E. ($n \geq 3$).

4. Discussion

Role of efflux transporters in drug absorption, distribution, metabolism, excretion and toxicology of various therapeutic agents is well acknowledged (Cummins et al., 2003; Katragadda et al., 2005). Considerable amount of research has been directed towards circumvention of these efflux proteins through rationale drug design (Crivori et al., 2006; Raub, 2006). However, structure activity relationship (SAR) for these efflux transporters is highly complex and poorly understood. One of the important reasons for this poor understanding is the wide substrate specificity and unavailability of 3-D protein structures of the efflux transporters. Of all the efflux pumps identified so far P-glycoprotein (P-gp) and multi drug resistance protein (MRP-2) have been shown to play important roles in drug absorption, distribution and elimination. In our previous reports we have demonstrated that peptide prodrug modifications of quinidine and SQV resulted in circumvention of P-gp mediated efflux (Jain et al., 2004, 2005, 2007). The primary objective of this study was to demonstrate whether the dipeptide conjugates of SQV can circumvent MRP-2 mediated efflux. HIV-PI is an important class of therapeutic agent for the management of HIV infection. It appears that almost all the PIs are substrates for MRP-2 efflux pump (Huisman et al., 2002; Williams et al., 2002; Agarwal et al., 2007). Overcoming the barrier presented by MRP-2 efflux pump will not only aid in enhancing drug absorption in gut but also may lead to increased drug permeability across various other biological barriers such as BBB (Park and Sinko, 2005).

Uptake studies in MDCKII-MRP2 cells suggest that in the presence of MK-571, a specific MRP-2 inhibitor, there is significant increase in the cellular accumulation of [^{3}H] SQV (Fig. 1). Enhancement in cellular accumulation may be due to inhibition of MRP-2 efflux process by MK-571. Such studies were also carried out with SQV and its prodrugs as inhibitors. In the presence of equimolar concentrations (50 μM) of SQV, Val-Val-SQV and Gly-Val-SQV, there was a significant increase in the cellular accumulation of [^{3}H] SQV. However, the extent of inhibition by prodrugs was much less relative to SQV (Fig. 1). This result confirmed that the prodrugs probably exhibit reduced affinity and are partially bypassing MRP-2 mediated efflux. Furthermore, uptake studies were conducted to study whether SQV prodrugs are substrates for peptide transporters. Uptake of [^{3}H] gly-sar (0.5 μCi/mL) was studied in the presence of unlabeled gly-sar, at concentrations of 2 and 5 mM. Results suggested a concentration dependent lowering in cellular accumulation of [^{3}H] gly-sar. Such diminished cellular uptake indicates expression of peptide transporters on the apical membrane of MDCKII-MRP2 cells (Fig. 2). Similar inhibition of [^{3}H] gly-sar uptake was also observed with Val-Val-SQV and Gly-Val-SQV indicating that the prodrugs possess high affinity for the peptide transporter expressed on MDCKII-MRP2 cells. Transepithelial transport studies were carried out across MDCKII-MRP2 cells to further investigate whether partial circumvention and partial utilization of peptide transporter, as seen in uptake studies, can result in enhanced transport across cell monolayer. Transport studies revealed that the SQV being a substrate for MRP-2 exhibits differential permeability in A → B and B → A direction (Fig. 3) with an efflux ratio of 7.4. However, this differential permeability effect is totally abolished in the presence of MK-571, a specific MRP-2 inhibitor (Fig. 3).

Transport of Gly-Val-SQV across MDCK-MRP2 cells demonstrated a slight increase in A → B permeability as compared to SQV (Fig. 4). However, such difference is not statistically significant. In the presence of MK-571 there is a significant elevation in the permeability values, of Gly-Val-SQV, in apical to basolateral (A → B) direction relative to SQV indicating that this prodrug display partial interaction with MRP-2 (Table 1). The efflux ratio of Gly-Val-SQV also diminished in the presence of MK-571 indicating that this peptide prodrug interacts with MRP-2 and is able to circumvent MRP-2 mediated efflux. However, similar transport studies with Val-Val-SQV show enhanced permeability in the A → B direction, which is not affected by MK-571 (Fig. 5), indicating that prodrug modification of SQV to Val-Val-SQV completely abolished its interaction with MRP-2 (Fig. 5). Finally, *in situ* single pass intestinal perfusion experiments were carried out to investigate the interaction of modified compounds in rat jejunum. In the basic SPIP experiment, the compound of interest is monitored in the perfusate only, not in the blood. Loss of compound is determined by the difference between the inlet and outlet concentrations and is attributed to absorption. Previous studies in buffer and intestinal homogenate suggested that the loss in outlet concentration is not due to metabolism of prodrugs during perfusion (Jain et al., 2007). Rat jejunal single pass intestinal perfusion experiments were performed in the presence and absence of MK-571 to study the interaction of the prodrugs with MRP-2. Permeability values and absorption rate constants of SQV and its prodrugs were carried out at steady state, which was confirmed by plotting the ratio of the outlet to inlet concentrations (corrected for water transport) versus time (Fig. 6). Val-Val-SQV and Gly-Val-SQV exhibited higher absorption rate constants and intestinal permeability coefficients as compared to SQV (Table 2). However, in the presence of MK-571 there was a significant increase in the absorption rate constant and intestinal permeability of SQV and Gly-Val-SQV (Fig. 7). In contrast there was no increase in the absorption rate constant and intestinal permeability of Val-Val-SQV in the, presence of MK-571, suggesting that Val-Val-SQV probably show no affinity for MRP-2. These results are consistent with the *in vitro* transport results where Val-Val-SQV showed no or very limited interaction with MRP-2. This differential interaction of Val-Val-SQV and Gly-Val-SQV can be attributed to their affinity towards peptide transport and/or MRP-2 efflux pump.

In conclusion, we have demonstrated that peptide prodrug modification of SQV to Val-Val-SQV and Gly-Val-SQV can lead to circumvention of MRP-2 mediated efflux. Gly-Val-SQV showed enhanced transport in the presence of MK-571 indicating that it is not fully circumventing MRP-2 mediated efflux process. However, *in vitro* and *in situ* results clearly demonstrated that prodrug modification of SQV to Val-Val-SQV completely abolished MRP-2 mediated efflux. Enhanced permeabilities of these agents can be attributed to a combination of peptide transporter mediated influx and circumvention of MRP-2 mediated efflux. Transporter targeted prodrug strategy may lead to shielding of drug molecules from various efflux pumps. Such an approach will aid not only in enhancing intestinal absorption but also distribution to other tissues such as brain, lungs and kidneys.

Acknowledgement

This work was supported by National Institute of Health Grant ROI AI 710099-01.

References

Agarwal, S., Pal, D., Mitra, A.K., 2007. Both P-gp and MRP2 mediate transport of Lopinavir, a protease inhibitor. Int. J. Pharm 339, 139–147.
Berggren, S., Hoogstraate, J., Fagerholm, U., Lennernas, H., 2004. Characterization of jejunal absorption and apical efflux of ropivacaine, lidocaine and bupivacaine in the rat using in situ and in vitro absorption models. Eur. J. Pharm. Sci. 21, 553–560.
Chiba, M., Hensleigh, M., Lin, J.H., 1997. Hepatic and intestinal metabolism of indinavir, an HIV protease inhibitor, in rat and human microsomes. Major role of CYP3A. Biochem. Pharmacol. 53, 1187–1195.
Crivori, P., Reinach, B., Pezzetta, D., Poggesi, I., 2006. Computational models for identifying potential P-glycoprotein substrates and inhibitors. Mol. Pharm. 3, 33–44.
Cummins, C.L., Salphati, L., Reid, M.J., Benet, L.Z., 2003. In vivo modulation of intestinal CYP3A metabolism by P-glycoprotein: studies using the rat single-pass intestinal perfusion model. J. Pharmacol. Exp. Ther. 305, 306–314.
Deeks, S.G., Smith, M., Holodniy, M., Kahn, J.O., 1997. HIV-1 protease inhibitors. A review for clinicians. JAMA 277, 145–153.
Dupre, J., Behme, M.T., Hramiak, I.M., McFarlane, P., Williamson, M.P., Zabel, P., McDonald, T.J., 1995. Glucagon-like peptide I reduces postprandial glycemic excursions in IDDM. Diabetes 44, 626–630.
Fagerholm, U., Johansson, M., Lennernas, H., 1996. Comparison between permeability coefficients in rat and human jejunum. Pharm. Res. 13, 1336–1342.
Fitzsimmons, M.E., Collins, J.M., 1997. Selective biotransformation of the human immunodeficiency virus protease inhibitor saquinavir by human small-intestinal cytochrome P4503A4: potential contribution to high first-pass metabolism. Drug Metab. Dispos. 25, 256–266.
Flexner, C., 1998. HIV-protease inhibitors. N. Engl. J. Med. 338, 1281–1292.
Haimeur, A., Conseil, G., Deeley, R.G., Cole, S.P., 2004. The MRP-related and BCRP/ABCG2 multidrug resistance proteins: biology, substrate specificity and regulation. Curr. Drug Metab. 5, 21–53.
Huisman, M.T., Smit, J.W., Crommentuyn, K.M., Zelcer, N., Wiltshire, H.R., Beijnen, J.H., Schinkel, A.H., 2002. Multidrug resistance protein 2 (MRP2) transports HIV protease inhibitors, and transport can be enhanced by other drugs. Aids 16, 2295–2301.
Issa, C., Gupta, P., Bansal, A.K., 2003. Implications of density correction in gravimetric method for water flux determination using rat single-pass intestinal perfusion technique: a technical note. AAPS PharmSciTech 4, E16.
Jain, R., Agarwal, S., Majumdar, S., Zhu, X., Pal, D., Mitra, A.K., 2005. Evasion of P-gp mediated cellular efflux and permeability enhancement of HIV-protease inhibitor saquinavir by prodrug modification. Int. J. Pharm. 303, 8–19.
Jain, R., Duvvuri, S., Kansara, V., Mandava, N.K., Mitra, A.K., 2007. Intestinal absorption of novel-dipeptide prodrugs of saquinavir in rats. Int. J. Pharm. 336, 233–240.
Jain, R., Majumdar, S., Nashed, Y., Pal, D., Mitra, A.K., 2004. Circumventing P-glycoprotein-mediated cellular efflux of quinidine by prodrug derivatization. Mol. Pharm. 1, 290–299.
Jansen, P.L., van Klinken, J.W., van Gelder, M., Ottenhoff, R., Elferink, R.P., 1993. Preserved organic anion transport in mutant TR-rats with a hepatobiliary secretion defect. Am. J. Physiol. 265, G445–452.
Katragadda, S., Budda, B., Anand, B.S., Mitra, A.K., 2005. Role of efflux pumps and metabolising enzymes in drug delivery. Expert Opin. Drug Deliv. 2, 683–705.
Kim, A.E., Dintaman, J.M., Waddell, D.S., Silverman, J.A., 1998a. Saquinavir, an HIV protease inhibitor, is transported by P-glycoprotein. J. Pharmacol. Exp. Ther. 286, 1439–1445.
Kim, R.B., Fromm, M.F., Wandel, C., Leake, B., Wood, A.J., Roden, D.M., Wilkinson, G.R., 1998b. The drug transporter P-glycoprotein limits oral absorption and brain entry of HIV-1 protease inhibitors. J. Clin. Invest. 101, 289–294.
Lee, C.G., Gottesman, M.M., 1998. HIV-1 protease inhibitors and the MDR1 multidrug transporter. J. Clin. Invest. 101, 287–288.
Lee, C.G., Gottesman, M.M., Cardarelli, C.O., Ramachandra, M., Jeang, K.T., Ambudkar, S.V., Pastan, I., Dey, S., 1998. HIV-1 protease inhibitors are substrates for the MDR1 multidrug transporter. Biochemistry 37, 3594–3601.
Lin, J.H., Chen, I.W., Vastag, K.J., Ostovic, D., 1995. pH-dependent oral absorption of L-735,524, a potent HIV protease inhibitor, in rats and dogs. Drug Metab. Dispos. 23, 730–735.
Lin, J.H., Chiba, M., Balani, S.K., Chen, I.W., Kwei, G.Y., Vastag, K.J., Nishime, J.A., 1996. Species differences in the pharmacokinetics and metabolism of indinavir, a potent human immunodeficiency virus protease inhibitor. Drug Metab. Dispos. 24, 1111–1120.
Morrow, C.S., Smitherman, P.K., Townsend, A.J., 2000. Role of multidrug-resistance protein 2 in glutathione S-transferase P1-1-mediated resistance to 4-nitroquinoline 1-oxide toxicities in HepG2 cells. Mol. Carcinog. 29, 170–178.
Mottino, A.D., Hoffman, T., Jennes, L., Vore, M., 2000. Expression and localization of multidrug resistant protein mrp2 in rat small intestine. J. Pharmacol. Exp. Ther. 293, 717–723.
Park, S., Sinko, P.J., 2005. P-glycoprotein and mutlidrug resistance-associated proteins limit the brain uptake of saquinavir in mice. J. Pharmacol. Exp. Ther. 312, 1249–1256.
Payen, L., Sparfel, L., Courtois, A., Vernhet, L., Guillouzo, A., Fardel, O., 2002. The drug efflux pump MRP2: regulation of expression in physiopathological situations and by endogenous and exogenous compounds. Cell Biol. Toxicol. 18, 221–233.
Polli, J.W., Jarrett, J.L., Studenberg, S.D., Humphreys, J.E., Dennis, S.W., Brouwer, K.R., Woolley, J.L., 1999. Role of P-glycoprotein on the CNS disposition of amprenavir (141W94), an HIV protease inhibitor. Pharm. Res. 16, 1206–1212.
Proust, V., Toth, K., Hulin, A., Taburet, A.M., Gimenez, F., Singlas, E., 2000. Simultaneous high-performance liquid chromatographic determination of the antiretroviral agents amprenavir, nelfinavir, ritonavir, saquinavir, delavirdine and efavirenz in human plasma. J. Chromatogr. B Biomed. Sci. Appl. 742, 453–458.
Rambaut, A., Posada, D., Crandall, K.A., Holmes, E.C., 2004. The causes and consequences of HIV evolution. Nat. Rev. Genet. 5, 52–61.
Raub, T.J., 2006. P-glycoprotein recognition of substrates and circumvention through rational drug design. Mol. Pharm. 3, 3–25.
Rost, D., Mahner, S., Sugiyama, Y., Stremmel, W., 2002. Expression and localization of the multidrug resistance-associated protein 3 in rat small and large intestine. Am. J. Physiol. Gastrointest. Liver Physiol. 282, G720–726.
Schapiro, J.M., Winters, M.A., Stewart, F., Efron, B., Norris, J., Kozal, M.J., Merigan, T.C., 1996. The effect of high-dose saquinavir on viral load and CD4+T-cell counts in HIV-infected patients. Ann. Intern. Med. 124, 1039–1050.
Su, Y., Zhang, X., Sinko, P.J., 2004. Human organic anion-transporting polypeptide OATP-A (SLC21A3) acts in concert with P-glycoprotein and multidrug resistance protein 2 in the vectorial transport of Saquinavir in Hep G2 cells. Mol. Pharm. 1, 49–56.
Sudoh, M., Pauletti, G.M., Yao, W., Moser, W., Yokoyama, A., Pasternak, A., Sprengeler, P.A., Smith 3rd, A.B., Hirschmann, R., Borchardt, R.T., 1998. Transport characteristics of peptidomimetics. Effect of the pyrrolinone bioisostere on transport across Caco-2 cell monolayers. Pharm. Res. 15, 719–725.
Sutton, S.C., Rinaldi, M.T., Vukovinsky, K.E., 2001. Comparison of the gravimetric, phenol red, and 14C-PEG-3350 methods to determine water absorption in the rat single-pass intestinal perfusion model. AAPS PharmSci 3, E25.
Ucpinar, S.D., Stavchansky, S., 2003. Quantitative determination of saquinavir from Caco-2 cell monolayers by HPLC-UV. High performance liquid chromatography. Biomed. Chromatogr. 17, 21–25.
Williams, G.C., Liu, A., Knipp, G., Sinko, P.J., 2002. Direct evidence that saquinavir is transported by multidrug resistance-associated protein (MRP1) and canalicular multispecific organic anion transporter (MRP2). Antimicrob. Agents Chemother. 46, 3456–3462.
Williams, G.C., Sinko, P.J., 1999. Oral absorption of the HIV protease inhibitors: a current update. Adv. Drug Deliv. Rev. 39, 211–238.
Wilson, M.E., Allred, K.F., Kordik, E.M., Jasper, D.K., Rosewell, A.N., Bisotti, A.J., 2007. Gender-specific effects of HIV protease inhibitors on body mass in mice. AIDS Res. Ther. 4, 8.
Wood, E., Hogg, R.S., Yip, B., Moore, D., Harrigan, P.R., Montaner, J.S., 2007. Superior virological response to boosted protease inhibitor-based highly active antiretroviral therapy in an observational treatment programme. HIV Med. 8, 80–85.